Carcinoma cellular uptake, imaging, and targeting by RGD- and TAT-conjugated upconversion and/or magnetic nanoparticles

D. Horák[*], U. Kostiv[*], V. Proks[*], D. Jirák[**]

[*]Institute of Macromolecular Chemistry, Academy of Sciences of the Czech Republic
Prague 162 06, Czech Republic, horak@imc.cas.cz
[**]Institute for Clinical and Experimental Medicine, Czech Republic

ABSTRACT

We have developed monodisperse magnetic Fe_3O_4, upconversion $NaYF_4$:Yb^{3+}/Er^{3+}, and dual paramagnetic/ upconversion $NaGdF_4$: Yb^{3+}/Er^{3+} nanoparticles with tunable size by thermal decomposition of Fe(III) oleate and lanthanide chlorides in high-boiling organic solvents. Aminosilica and 4-pentynoic acid were then introduced on the particle surface to conjugate the cell adhesive and cell penetrating RGD and TAT peptides, respectively. Optionally, $NaYF_4$:Yb^{3+}/Er^{3+}@SiO_2-NH_2 particles reacted with methoxyPEG succinimidyl ester to diminish uptake of the particles by the reticulo-endothelial system. Neural stem cell viability and labeling efficiency of the particles were determined. Al carboxyphthalocyanine was conjugated to $NaYF_4$:Yb^{3+}/Er^{3+}@SiO_2-PEG nanoparticles, which were intravenously administered in athymic nude mice with xenotransplanted human prostate carcinoma PC-3. After NIR photodynamic therapy, the tumor subsided and its volume approached to zero.

Keywords: upconversion nanoparticles, magnetic nanoparticles, carcinoma, peptide, photodynamic therapy

1 INTRODUCTION

Design of a versatile multifunction nanomaterial with proper magnetic and/or optical properties, which can simultaneously implement both diagnostic and therapeutic functions, is a long-lasting challenge in the current biomedical research. Imaging-guided drug delivery, facilitating the integration of diagnosis and treatment, can also greatly promote the study of particle/cell interaction. In this respect, superparamagnetic Fe_3O_4, upconversion $NaYF_4$:Yb^{3+}/Er^{3+}, and bimodal paramagnetic/upconversion $NaGdF_4$:Yb^{3+}/Er^{3+} nanoparticles seem to be promising as a new generation of multifunctional materials for magnetic resonance imaging (MRI), drug and gene delivery, biolabeling, luminescence imaging, hyperthermia, and photodynamic therapy (PDT).

PDT is an effective non-invasive phototherapeutic clinical approach for early-stage cancer and an adjuvant treatment for late-stage cancer after surgery involving photochemical reactions mediated by the interaction of nontoxic photosensitizers (e.g., phthalocyanine PC) with specific light and molecular oxygen. Upon irradiation by light with the appropriate wavelength, a photosensitizer is excited from a ground-state to a high-energy state, leading to energy transfer to neighboring molecular oxygen or other substrate molecules, causing the generation of cytotoxic singlet oxygen ($^1O_2$) or interacting with biological components and inducing cells to form other reactive oxygen species. PDT has a potential to localize tumor and treat it with high specificity, selectivity, and almost no side effects. In addition, when the photosensitizer, upon excitation, is able to produce fluorescence emission, it can act as both a therapeutic and imaging agent. Most of the currently available organic sensitizers are activated by either visible (400–700 nm) or UV light, which have very poor tissue penetration depths and cause photodamage of the living tissue. The biological tissues have relative transparency at 700-900 nm, nevertheless in the microvasculature the most abundant chromophore the blood hemoglobin absorbs the penetrating photons [1]. The penetration depth of visible light in living tissue is typically <3 mm [2]. To overcome this drawback, near-infrared (NIR)-excitable upconversion nanoparticles serve as a transducer by converting low energy NIR photons to upconversion photoluminescence enabling penetration of light into biological tissue to 10 mm and more [3]. The nanoparticles then emit visible luminescence via an energy transfer upconversion process, and have a great potential as a novel NIR-triggered PDT nanoplatform in deep tissue cancer therapy.

Surface engineering of the particles is of key importance to render the originally hydrophobic particles with hydrophilicity and dispersibility in aqueous media. At the same time, it substantially prolongs the blood circulation time, endows the particles with reactive groups (COOH, NH_2, SH) to facilitate subsequent biofunctionalization and coupling with many biomolecules, therapeutic agents, and enhances the active targeting efficiency maximizing the corresponding accumulation within tumors. Specific targeting and *in vivo* visualization of cancer cells is additional crucial point for early detection and treatment of cancer. Modification of the particles by functional targeting moieties (e.g., peptides, antibodies) can greatly improve the efficiency of PDT. Immobilization of cell-adhesive tripeptide Arg-Gly-Asp **(**RGD) derived from fibronectin considerably promotes the particle adhesion to the cell

membrane through integrins present on the cell surface. In contrast to RGD, the arginine-rich transcription activator (TAT) of the human immunodeficiency virus type 1 (HIV-1), known as the first cell-penetrating peptide (CPP), makes efficient entering of HIV in the cells. TAT peptide thus supports delivery of the nanoparticles into any cell type.

In this work, monodisperse Fe_3O_4, $NaYF_4$:Yb^{3+}/Er^{3+}, and $NaGdF_4$:Yb^{3+}/Er^{3+} nanoparticles were designed and modified by a thin silica shell. To render the particles with a targeting moiety, RGD- or TAT-based peptides were synthesized and immobilized on the nanoparticle surface via Cu(I)-catalyzed Huisgen azide-alkyne click cycloaddition. Al carboxyphthalocyanine (Al PC) was conjugated to the upconversion nanoparticles via carbodiimide chemistry. *In vitro* cytotoxicity and intracellular uptake of the nanoparticles were tested with human cervical carcinoma HeLa cells. *In vivo* Al PC-conjugated upconversion nanoparticles were tested for PDT with athymic nude mice inoculated with xenotransplanted human prostate carcinoma PC-3 after illumination with NIR light; the magnetic particles were then tested in MRI.

2 EXPERIMENTAL

Monodisperse Fe_3O_4, $NaYF_4$:Yb^{3+}/Er^{3+}, and $NaGdF_4$:Yb^{3+}/Er^{3+} nanoparticles stabilized with oleic acid were obtained by thermal decomposition of Fe(III) oleate and lanthanide chlorides. The particle surface was modified by a thin homogeneous silica/aminosilica shell using hydrolysis and condensation of tetramethyl orthosilicate and (3-aminopropyl)triethoxysilane and water-in-oil reverse microemulsion technique [4, 5]. Aminosilica-coated Fe_3O_4, $NaYF_4$:Yb^{3+}/Er^{3+}, and $NaGdF_4$:Yb^{3+}/Er^{3+} particles were then modified with poly(ethylene glycol) (PEG) succinimidyl ester.

$NaYF_4$:Yb^{3+}/Er^{3+}@SiO_2-NH_2 nanoparticles were reacted with 4-pentynoic acid and subsequently with azidopentanoyl-RGD and azidopentanoyl-TAT peptides via Cu(I)-catalyzed click cycloaddition [6]. As the RGD peptide is amenable to radiolabeling, its concentration on the nanoparticle surface was determined by labeling with ^{125}I-isotope. Because Cu(I) catalyst is considered as toxic, amount of adsorbed residual Cu(I) catalyst on the nanoparticle surface after the click reaction was determined by ^{64}Cu(I)-isotope radioassay. Finally, Al carboxy-phthalocyanine (Al PC) was coupled to $NaYF_4$:Yb^{3+}/Er^{3+}@SiO_2-PEG particles by 1-ethyl-3-(3-dimethylaminopropyl)carbodiimide and *N*-hydroxysuccin-imide.

Physicochemical properties of the nanoparticles were determined by transmission electron microscopy to analyze the morphology, size, and particle size distribution. Hydrodynamic particle diameter and ζ-potential were measured by dynamic light scattering. ATR FT-IR spectroscopy and elemental analysis were used to investigate the nanoparticle surface and composition. X-ray and selected area electron diffraction on TEM microscope verified the crystal structure of the particles. To identify an optimal excitation wavelength with a high intensity of emitted light, the nanoparticle upconversion emission was measured at 500-700 nm with excitation ranging from 930 to 990 nm. Maximum absorption was observed at 970 nm, corresponding to the $^2F_{7/2}$ - $^2F_{5/2}$ transition of Yb^{3+}. Under this excitation, the upconversion emission displayed three peaks at 520, 545 (both green), and 660 nm (red), which corresponded to the $^2H_{11/2}$ - $^4I_{15/2}$, $^4S_{3/2}$ - $^4I_{15/2}$, and $^4F_{9/2}$ - $^4I_{15/2}$ transitions of Er^{3+}, respectively.

In vitro biocompatibility and biosafety of the particles was investigated using murine neural stem cells in terms of oxidative stress response and cell viability, proliferation, and uptake. The particles were incubated with human cervical carcinoma HeLa cells, stained by mRoGFP and CellMask™ Orange plasma membrane dye, and monitored using a Leica TCS SP2 AOBS confocal inverted fluorescence microscope and a Coherent Chameleon Ultra Ti:Sapphire laser at 970 nm. MRI of the particle-labelled cells was performed by 4.7 T Bruker BioSpec spectrometer.

3 RESULTS AND DISCUSSIONS

We have developed monodisperse PEG-modified SiO_2-coated superparamagnetic Fe_3O_4 nanoparticles with a spherical shape and size tuned from 6 to 20 nm (Figure 1 a).

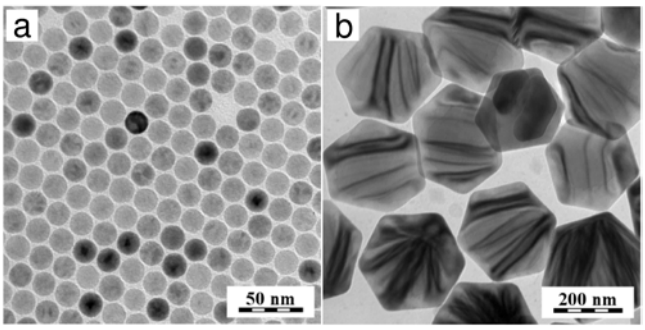

Figure 1. TEM micrographs of (a) spherical superparamagnetic Fe_3O_4 and (b) hexagonal upconversion $NaYF_4$:Yb^{3+}/Er^{3+} nanoparticles.

Similarly, novel monodisperse spherical or hexagonal upconversion $NaYF_4$:Yb^{3+}/Er^{3+} and paramagnetic $NaGdF_4$:Yb^{3+}/Er^{3+} nanoparticles with size controlled in 16-266 nm range were obtained by oleic acid-stabilized thermal decomposition of lanthanide chlorides in the presence of NaF (Figure 1 b). Advantage of this method consists in the formation of particles with a narrow size distribution, high phase purity, magnetic and luminescent efficiency. It is not necessary to note, that the tunable particle size and uniformity, as well as the reproducibility of the synthesis, are of critical importance for prospective bioapplications.

In general, nanoparticles synthesized in the presence of organic capping ligands are poorly dispersible in aqueous media, which limits their usage in medicine. To render the originally hydrophobic particles with hydrophilic properties, the surface has to be further modified. In this

respect, biocompatible, optically transparent, chemically inert, and thermally stable silica shell, which contains high surface area available for loading of required drugs, has many advantages as a coating material. It also serves as a support for additional modifications to introduce functional groups, such as amino, carboxyl, and methacrylate, for the prospective attachment of biomolecules and polymers. Aminosilica shell was therefore introduced on the particle surface, which was followed by a reaction with 4-pentynoic acid and conjugation of the $NaYF_4:Yb^{3+}/Er^{3+}@SiO_2$-alkyne particles with azido-functionalized cell-adhesive RGD and cell-penetrating TAT peptide. This provided a new generation of biomimetic luminescent biomarkers, which target cell nucleus and/or membrane (Figure 2). RGD is a well-known cell-adhesive amino acid sequence, which preferentially interacts with the cell membrane via its integrins to specifically target cancer cells. In contrast, the cell-penetrating TAT peptide derived from the HIV-1 TAT protein enables the nanoparticles to cross the cell membrane and enter the cytoplasm.

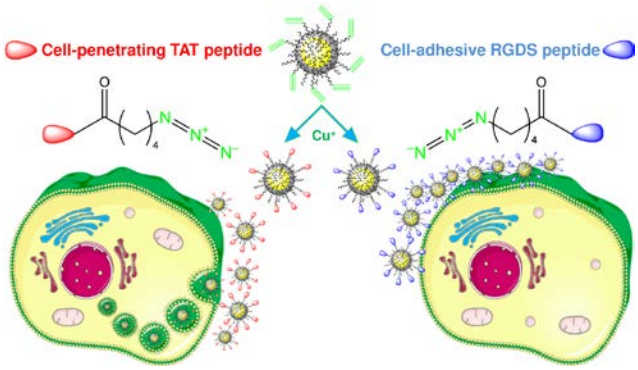

Figure 2. (a) Schematic illustration of $NaYF_4:Yb^{3+}/Er^{3+}@SiO_2$-alkyne nanoparticle conjugation with TAT and RGD peptides and their cell interaction.

Specific targeting and uptake of the RGD- and TAT-conjugated $NaYF_4:Yb^{3+}/Er^{3+}@SiO_2$ nanoparticles by human cervix carcinoma HeLa cells was monitored by confocal microscopy. While $NaYF_4:Yb^{3+}/Er^{3+}@SiO_2$-TAT particles predominantly crossed the cell membrane and accumulated in the cell cytoplasm (Figure 3 a), the $NaYF_4:Yb^{3+}/Er^{3+}@SiO_2$-RGD particles were localized mainly on the cell plasma membrane due to specific binding of the peptide to the corresponding integrins (Figure 3 b). Excellent visibility and facile monitoring of the RGD- and TAT-conjugated $NaYF_4:Yb^{3+}/Er^{3+}$ nanoparticles in the living cells is very promising for perspective use of these new drug-conjugated upconversion nanoparticles in theranostic applications enabling targeting and imaging of specific tumor phenotypes.

$NaYF_4:Yb^{3+}/Er^{3+}$ nanoparticles have also attracted a lot of attention as a promising photosensitizer carrier for a deep tissue PDT. The aminosilica-coated nanoparticles were therefore conjugated with Al PC via carbodiimide chemistry. Red emission (640-680 nm) of the excited upconversion particles matches very well with the excitation of Al PC (650-680 nm). Due to a large specific surface area and insufficient colloidal stability, $NaYF_4:Yb^{3+}/Er^{3+}@SiO_2$-PC nanoparticles had a tendency to non-specifically adsorb proteins from blood plasma, which inevitably led to undesirable particle aggregation. As a result, the particles could be rapidly shuttled out of the blood circulation and internalized by macrophages and endothelial cells of the reticuloendothelial system, in

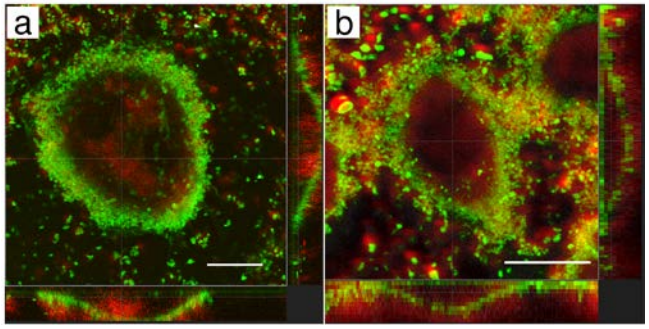

Figure 3. Fluorescence images of cell sections and upconversion photoluminescence of (a) $NaYF_4:Yb^{3+}/Er^{3+}@SiO_2$-TAT- and (b) $NaYF_4:Yb^{3+}/Er^{3+}@SiO_2$-RGD-labeled HeLa cells after CellMask™ orange staining. Cell plasma membrane is green (excitation and detection at 540 and 565 nm, respectively) and nanoparticles are red (excitation and detection at 970 and 500-700 nm, respectively). Scale bar 20 µm.

particular by the liver and spleen. To obtain not only a stable colloid without particle aggregation, but also to prevent undesirable protein adsorption and to prolong half-life time in the blood circulation, the nanoparticle surface was further modified by PEG. It is considered as a very promising biomedical material, that protects the nanoparticles from the immune system, promotes a longer circulation time, and inhibits removal by the reticuloendothelial system. Moreover, PEG is inexpensive and FDA-approved for a wide range of bioapplications. Therefore, the $NaYF_4:Yb^{3+}/Er^{3+}@SiO_2$-PC nanoparticles were further modified by methoxyPEG succinimidyl ester to form a novel system for *in vivo* deep tissue PDT triggered by NIR light. Upon 970 nm irradiation, intensive red emission of the $NaYF_4:Yb^{3+}/Er^{3+}@SiO_2$-PEG-PC nanoparticles completely vanished indicating efficient energy transfer from the nanoparticles to Al PC forming $^1O_2$. $^1O_2$ generation was measured on a model system based on human HeLa cells. Finally, $NaYF_4:Yb^{3+}/Er^{3+}@SiO_2$-PEG-PC particles were intravenously administered in athymic nude mice with xenotransplanted human prostate carcinoma PC-3 (Figure 4 a). The tumor necrotized after PDT using a 970-nm laser (Figure 4 b).

Moreover, we have synthetized $NaGdF_4:Yb^{3+}/Er^{3+}$ nanoparticles combining upconversion emission with MRI and external magnetic manipulation. Integration of these two modalities (paramagnetic/upconversion) into one particle renders the system with potential applications in photothermal therapy and PDT, MRI, and biosensing.

Figure 4. (a) Athymic nude mice with xenotransplanted human PC-3 tumor 48 h after experimental NIR PDT (970 nm, 160 J/cm^2) performed 20 min after intravenous injection of $NaYF_4$:Yb^{3+}/Er^{3+}@SiO_2-PEG-PC nanoparticles (0.5 mg per 100 µl). (b) Necrotized tumor.

4 CONSCLUSIONS

Monodisperse superparamagnetic, upconversion, and bimodal paramagnetic/upconversion nanoparticles were successfully synthesized. The particles were found to be a suitable theranostic agent with superior magnetic properties and bright luminescence. To facilitate nanoparticle dispersibility in water, they were coated by silica/aminosilica via a reverse microemulsion technique and further conjugated with PEG succinimidyl ester through amide bond formation. Uptake of PEGylated nanoparticles by murine neural stem cells was lower than that of silica-coated particles, which was in agreement with literature describing that PEG protects the particles from the immune cell system. Biocompatibility evaluation demonstrated that PEGylated and silica-coated nanoparticles did not induce cytotoxicity, although slight disturbances in the cell function leading to ROS production, mitochondrial depolarization, and activation of antioxidative defense mechanisms may occur either upon internalization or contact of the nanoparticles with the cells.

To achieve high uptake of magnetic and/or luminescent particles by cancer cells, active targeting was designed using immobilization of biorecognition molecules on the nanoparticle surface. Cell adhesive and cell penetrating azidopentanoyl-RGD and azidopentanoyl-TAT peptide was conjugated to the particles. The experiments with the HeLa cells demonstrated that the $NaYF_4$:Yb^{3+}/Er^{3+}@SiO_2-RGD and $NaYF_4$:Yb^{3+}/Er^{3+}@SiO_2-TAT particles differed in their cell interaction mechanisms. While the $NaYF_4$:Yb^{3+}/Er^{3+}@SiO_2-RGD particles adhered to the cell plasma membrane, the $NaYF_4$:Yb^{3+}/Er^{3+}@SiO_2-TAT nanospheres were specifically targeted to the cell cytosol. Targeting to the cell cytosol and/or plasma membrane may be exploited in different biomedical applications, including drug delivery. As an example, active targeting of the $NaYF_4$:Yb^{3+}/Er^{3+}@SiO_2-RGD particles to the cell plasma membrane could be a prospective tool for *in vivo* cell imaging, whereas targeting of the $NaYF_4$:Yb^{3+}/Er^{3+}@SiO_2-TAT nanoparticles to the cytosol might be suitable for PDT or photothermal therapy. Moreover, $NaYF_4$:Yb^{3+}/Er^{3+}@SiO_2-RGD and $NaYF_4$:Yb^{3+}/Er^{3+}@SiO_2-TAT nanoparticles may be promising for the design of novel multifunctional bioconjugates for the specific noninvasive targeting and recognition of tumor cells. Prospectively, the conjugation of RGD- and TAT-immobilized upconversion nanoparticles with additional ligands (e.g., monoclonal antibody) might provide a new method for the production of theranostic agents that are specific to tumor cell phenotypes.

New drug prototype based on $NaYF_4$:Yb^{3+}/Er^{3+}@SiO_2-PEG-PC nanoparticles with highly efficient generation of cytotoxic $^1O_2$ upon NIR excitation was designed. These upconversion nanoparticles convert low-energy NIR irradiation into higher-energy emissions allowing thus PDT in tissues. The excellent antitumor effect of the $NaYF_4$:Yb^{3+}/Er^{3+}@SiO_2-PEG-PC nanoparticles in mouse model with xenotransplanted human prostate carcinoma PC-3 demonstrated their great potential as a novel drug delivery system for *in vivo* NIR-triggered PDT of cancer. Paramagnetic/upconversion nanoparticles modified with a specific targeting peptide and photosensitizer then hold promise not only for cancer therapy by PDT, but also for MRI and luminescent imaging. This integration of several possible individual treatments and imagings into a single nanotheranostic platform will enable multimodal synergetic therapy and bioimaging accurately quantifying nanoparticle accumulation in various major organs *in vivo*.

Acknowledgement. Financial support of the Czech Science Foundation (No. 15-01897S) and the International Research and Innovation in Medicine Program at Cedars-Sinai Medical Center and the Regional Cooperation in Health, Science and Technology (RECOOP) Association is acknowledged.

REFERENCES

[1] J.M. Maarek, S.G. Vari, L. Marcu, T. Papaioannou, V.R. Pergadia, W.J. Snyder and W.S. Grundfest, SPIE Proc. 2135, 157, 1994.

[2] K.R. Byrnes, R.W. Waynant, I.K. Ilev, X. Wu, L. Barna, K. Smith, R. Heckert, H. Gerst and J.J. Anders, Lasers Surg. Med. 36, 171, 2005.

[3] L. Liang, Y. Lu, R.Zhang, A. Care, T.A. Ortega, S.M. Deyev, Y. Qian and A.V. Zvyagin, Acta Biomaterialia http://dx.doi.org/10.1016/j.actbio.2017.01.004

[4] U. Kostiv, V. Patsula, M. Šlouf, I. Pongrac, S. Škokić, M. Radmilović, I. Pavičić, I. Vinković Vrček, S. Gajović and D. Horák, RSC Advances 7, 8786, 2017.

[5] U. Kostiv, O. Janoušková, M. Šlouf, N. Kotov, H. Engstová, K. Smolková, P. Ježek and D. Horák, Nanoscale 7, 18096, 2015.

[6] U. Kostiv, I. Kotelnikov, V. Proks, M. Šlouf, J. Kučka, H. Engstová, P. Ježek and D. Horák, ACS Appl. Mater. Interfaces 8, 20422, 2016.